ChemPubSoc Europe

DOI: 10.1002/chem.201503430

CHEMISTRY A European Journal Full Paper

Fluorenes

Tuning the Electronic Properties of Acetylenic Fluorenes by Phosphaalkene Incorporation

Yurii V. Svyaschenko, Andreas Orthaber,* and Sascha Ott*[a]

Abstract: Versatile synthetic protocols for 2,7- and 3,6-diacetylenic fluorene-9-ylidene phosphanes (F9Ps) were developed. Protodesilylation of trimethylsilyl-protected acetylenic F9Ps affords terminal acetylenes that can be employed in Sonogashira and Glaser-type C–C coupling reactions to give thienyl-decorated and butadiyne-bridged fluorene-9-ylidene phosphanes, respectively. As evidenced by UV/Vis spectroscopy and cyclic voltammetry and corroborated by ab initio calculations, the presence of the P center in the F9Ps induces a significantly reduced HOMO–LUMO splitting that originates from stabilization of the LUMO levels. Variation of the acetylene substitution pattern is an additional tool to influence the optical and electronic properties. Whereas 3,6-disubstituted F9Ps have strong absorptions around 400 nm, mainly due to π–π^* transitions, 2,7-diacetylenic F9Ps exhibit longest-wavelength absorptions that have significant charge-transfer character with an onset around 520 nm.

Introduction

Carbon-rich compounds that have an extended π-conjugated system have been widely investigated as materials in electronic and photonic applications,[1] and well defined one-, two-, and three-dimensional molecular architectures have been prepared for such purposes.[2] The effective conjugation path can be expanded by locking aryl groups into coplanarity to decrease their rotational freedom and to maximize orbital overlap. Fluorenes in which two phenyl groups of a biphenyl are tied together with a methylene bridge are a prominent example of this strategy. As one of the most powerful building blocks in organic electronics,[3] fluorenes have been incorporated into linear[4] and cyclic oligomers (radialenes),[5] blue-emitting copolymers,[6] metal–organic hybrid polymers,[7] self-assembled π stacks,[8] and purely organic polymers.[9] In addition, fluorene derivatives have recently been used as building blocks for conductive polymers in organic thin-film transistor applications[10] and photovoltaics.[11] Functionalization of fluorenes is often achieved through coupling of halogenated precursors (mainly in 2,7- and 3,6-positions)[12] or exploiting the acidity of the 9-H position.[13] The latter approach is commonly used for the introduction of solubilizing groups such as long alkyl chains that control aggregation in solution or the solid state.[14] Changing from a CH_2 (or CR_2) bridge in fluorenes to fluorenones (C=O) or 9-methylidene fluorenes ($C{=}CR_2$) can lead to significant alterations of the optoelectronic properties.[12b,15] Moreover, recent studies on diacetylenic 9-dicyanomethylene fluorenes and fluorenones with electron-rich carbazole substituents at the acetylenic termini have shown that variation of the substitution pattern can also have an impact on the donor–acceptor properties (Figure 1 a, b).[12b,15b]

An alternative approach to conjugated materials with unprecedented properties is heteroelement incorporation. The use of main group elements as p-type dopants has recently led to extraordinary examples of π-conjugated materials with small bandgaps[16] and materials with interesting bonding situations.[17] Especially the chemistry of organophosphorus π-conjugated materials has seen considerable development in recent years, with the synthesis of novel P-based conjugated compounds and the elucidation of their optical and electrochemical properties.[16d,18] Fascinating phosphaalkene architectures have been prepared and investigated, such as a benzene with multiple phosphaethene substituents,[19] linear poly- and oligomers,[20] and radialenes[21] with endo- and exotopic phosphaalkene units. Over the last decades, attempts have been made to investigate the influence of phosphorus incorporation into the exocyclic double bond of fluorene-9-ylidene phosphanes (F9Ps)[22] and their allenic congeners.[23] Whereas P incorporation generally has a profound effect on the properties of the compounds, additional variations of the *P*-substituents gives only minor alterations in the optoelectronic properties of the heterofluorenes.[24] Radical anions of F9P derivatives have been prepared electrochemically and chemically, and their stability is rationalized by a resonance structure with a phosphinyl radical and an anionic fulvene.[25]

In the present work, we studied the impact of heteroelement incorporation, in the form of phosphaalkenes, on acetylene-extended fluorene frameworks. Moreover, the impact of the rigid core was investigated and compared to *C,C*-diphenyl (phospha)alkenes. Inspired by previous works, different acety-

[a] Dr. Y. V. Svyaschenko, Dr. A. Orthaber, Prof. Dr. S. Ott
Department of Chemistry - Ångström Laboratory
Uppsala University, Box 523, 75120 Uppsala (Sweden)
E-mail: Andreas.Orthaber@kemi.uu.se
Sascha.Ott@kemi.uu.se

Supporting information for this article is available on the WWW under http://dx.doi.org/10.1002/chem.201503430.

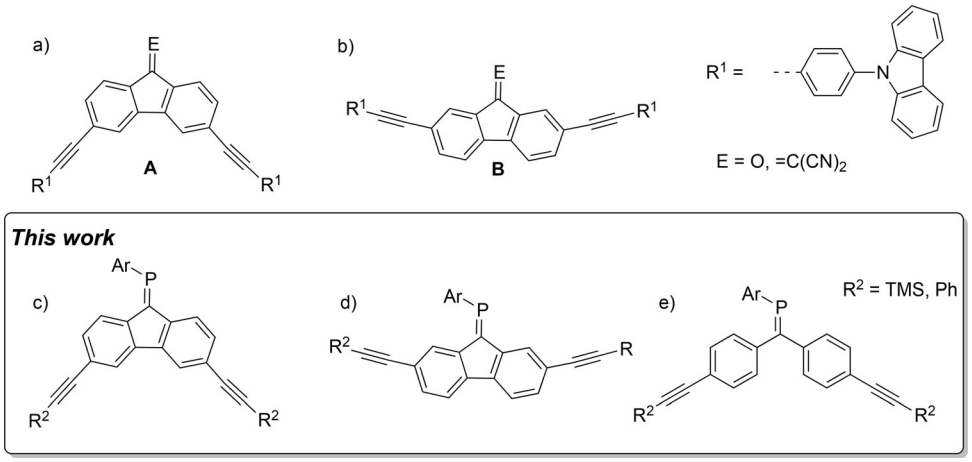

Figure 1. Examples of 3,6- (**A**) and 2,7-diacetylene substituted fluorenes (**B**) with carbazole donor termini (a, b). Studied F9Ps (c, d) and nonlocked *C*,*C*-diphenyl phosphaalkene reference compounds (e).

lene substitution patterns were investigated to give insights into the bonding situation and the effect of the carbon–phosphorus exchange on the frontier molecular orbitals. In this work, we sought to combine phosphaalkenes, fluorenes, and oligoacetylenes to afford a new class of planar π-conjugated compounds with significantly smaller HOMO–LUMO gaps and demonstrate their synthetic scope as building blocks for the construction of future π-conjugated materials.

Results and Discussion

Synthesis

Several approaches can be envisaged for the synthesis of acetylenic F9Ps, which mainly differ in the order in which the different substituents are introduced at the fluorene core. For most of the compounds described herein, it turned out to be more efficient to assemble the acetylenic fluorene framework first, and then introduce the unsaturated phosphorus fragment. Thus, acetylenic fluorenes **2a**,**b** and **3a**,**b** were first prepared by Sonogashira cross-coupling reactions from 3,6-dibromofluorene (**1a**) and 2,7-dibromofluorene (**1b**; Scheme 1). Whereas **1b** is commercially available, **1a** had to be prepared in six steps from 9,10-phenanthrenequinone by a modified literature procedure (see the Supporting Information).[12c]

The phosphane can easily be introduced on the diacetylenic fluorenes **2**,**3** by treatment with *n*BuLi and addition of the resulting Li salt to a solution of Mes*PCl_2 (Mes* = 2,4,6-tri-*tert*-butylphenyl) to give chlorophosphanes **4a**,**b** and **5a**,**b**, which were characterized by ^{31}P NMR spectroscopy and used without further purification. Dehydrochlorination with the non-nucleophilic base 1,8-diazabicyclo[5.4.0]undec-7-ene (DBU) established the P=C bond and completed the synthesis of **6**,**7** in modest to good overall yields (16–84%).

In the case of **7a**,**b**, it is possible to protodesilylate the acetylene termini, which can then be further elaborated by desirable substituents to fine-tune the photophysical and electrochemical properties of the F9Ps.[20e,f,26] The feasibility of such

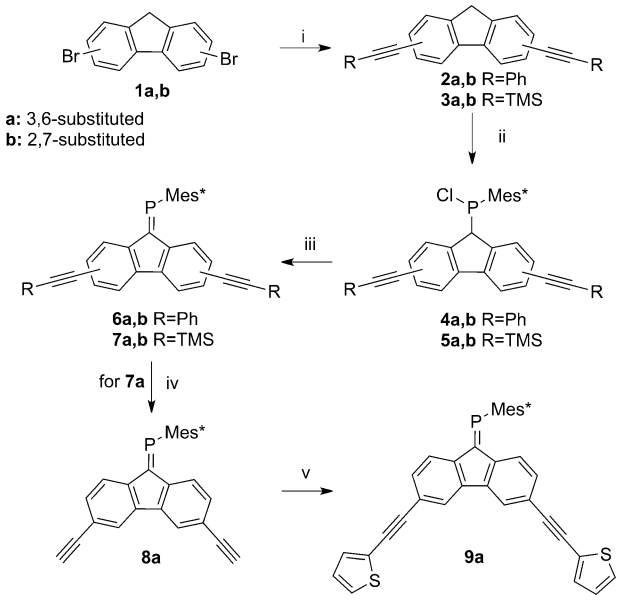

Scheme 1. i) RC≡CH, 80 °C, CuI, $[PdCl_2(PPh_3)_2]$, toluene/*i*Pr_2NH, overnight; ii) *n*BuLi, −78 °C, Mes*PCl_2, THF, 1 h; iii) DBU, 2 h; iv) K_2CO_3, MeOH, THF, 30%; v) 2-Iodothiophene, THF, MeOH, CuI, $[PdCl_2(PPh_3)_2]$, RT, 38%.

a strategy was exemplified by the deprotection of phosphaalkene **7a** with K_2CO_3 and isolation of the terminal bis-acetylene **8a**. The latter compound engages in Sonogashira cross-coupling reactions, for example, with 2-iodothiophene to afford **9a** (Scheme 1).

In addition, phosphaalkenes with a dihalo-substituted fluorene core as in **12** and monohalo-substituted fluorenes **15** and **16** were targeted. These compounds are appealing monomers for the synthesis of π-conjugated conductive materials,[27] oligomers, or macrocycles,[13] since they could engage in other C–C cross-coupling reactions such as Yamamoto or Suzuki coupling. Dibromofluorenes **1a**,**b** can be easily lithiated at −78 °C to give the corresponding lithium salts, which react with Mes*PCl_2 with formation of chlorophosphanes **11a**,**b**. The reac-

tion was monitored by ^{31}P NMR spectroscopy and, after completion, the resulting intermediates **11** were treated with DBU, as described above, to afford dibromofluorenes **12a,b** in good yields (Scheme 2). A constant low temperature (below −70 °C) during lithiation plays a critical role in this reaction. If the temperature is allowed to exceed −40 °C, formation of sizeable amounts of presumably polymeric side products that complicate purification is observed.

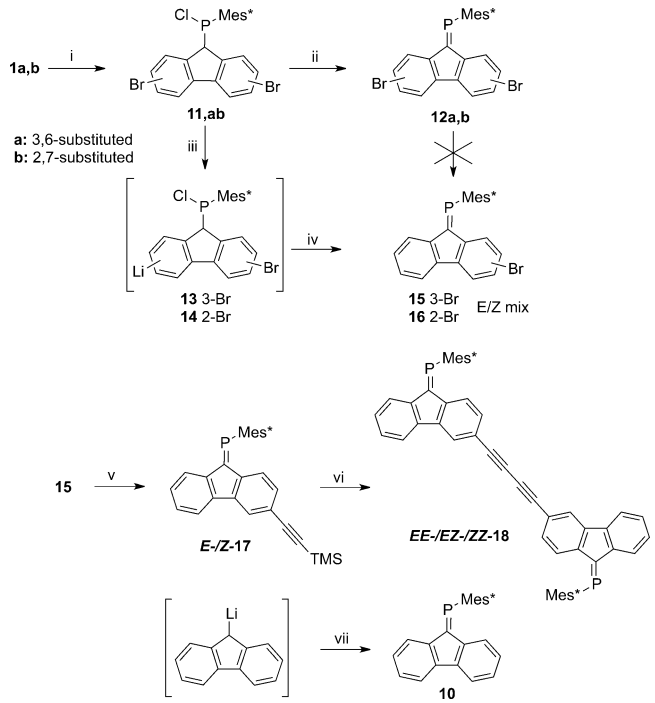

Scheme 2. Synthesis of substituted fluorene-9-ylidene phosphanes. i) *n*BuLi, −78 °C, Mes*PCl_2, THF, 1 h; ii) DBU, 2 h; iii) *n*BuLi, −78 °C, 5 min; iv) DBU, 2 h; v) RC≡CH, 80 °C, CuI, [$PdCl_2(PPh_3)_2$], toluene/*i*Pr_2NH, overnight, 75%; vi) pyridine, MeOH, $Cu(OAc)_2$, K_2CO_3, 77%; vii) 1) Mes*PCl_2, THF, 1 h; 2) DBU, 2 h.

Asymmetric monobromofluorenes **15** and **16** were targeted from dibromofluorenes though lithium/bromide exchange reactions, followed by protonation. Interestingly, treatment of phosphaalkene-containing dibromofluorene **12** with *n*BuLi and subsequent quenching with water did not afford any monobrominated fluorene, but resulted in the formation of a complex mixture of polymeric materials that most likely stem from initial attack of BuLi at the P=C unit.[16c,28] However, addition of *n*BuLi to chlorophosphanes **11a,b**, followed by treatment with DBU and subsequent aqueous workup affords monobromofluorenes **15**,**16** as a mixture of *E*/*Z* isomers in a ratio of about 1:1 in good total yields (Scheme 2). Prolonged lithiation leads to significantly lower yields and increased amounts of unsubstituted F9P **10**. Attempts to separate *E*/*Z* isomers were not successful, since the two isomers interconvert to restore the initial equilibrium within 1 d under ambient conditions.

The synthetic versatility of the monohalogenated precursors was demonstrated by the preparation of dimeric compound **18**. Starting from **15**, Sonogashira coupling with trimethylsilylacetylene (TMS-acetylene) gave monoacetylenic F9P **17** as a mixture of *E*/*Z* isomers. In situ deprotection of the mixture of isomers with K_2CO_3, followed by Glaser-type coupling, afforded butadiyne-bridged dimeric **18** as a mixture of *EE*, *EZ*, and *ZZ* isomers, with the *ZZ* isomer being the main product of about 50%, as determined by ^{31}P NMR spectroscopy. Recrystallization from pentane gave a single compound, which was assigned as the *ZZ* isomer on the basis of the characteristic ^{1}H NMR shift ($\delta = 4.90$ ppm) of H1, which lies directly under the Mes* fragment,[29] and the expected dd coupling pattern (see Supporting Information).

To compare the effect of the different functional groups at the fluorene core, that is, the phosphaalkene and the acetylenes at different positions, as well as the influence of the fluorene itself, a number of different reference compounds were synthesized. Fluorene **10**,[22c] which lacks the acetylene units, was prepared from lithiated fluorene by following the typical reaction sequence with dichlorophosphane followed by dehydrohalogenation with DBU (Scheme 2).

C,*C*-Diphenyl phosphaalkenes **23** and **24**, which lack the central bond of the fluorene core, were synthesized by a similar approach. Chlorophosphanes **21**,**22** were generated by lithiation of **19** and **20**, followed by reaction with Mes*PCl_2 in THF. Surprisingly, dehydrohalogenation to give the targeted phosphaalkenes was found to be very sluggish, and even heating the reaction mixture in the presence of DBU to reflux in THF (66 °C) for several hours did not convert the starting materials. Under even harsher conditions, phosphaalkenes **23** and **24** could finally be obtained from their corresponding chlorophosphanes **21** and **22** in refluxing toluene (111 °C) after 2 d (Scheme 3).

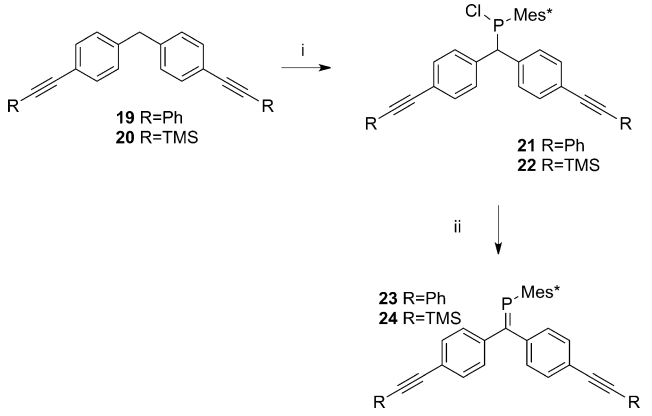

Scheme 3. Synthesis of acetylene-substituted *C*,*C*-diphenyl phosphaalkenes. i) *n*BuLi, −78 °C, Mes*PCl_2, THF, 1 h; ii) DBU, toluene, reflux, 2 d.

Fundamental to our study are possibilities to determine the influence that the phosphorus center exerts on the overall π system and, in order to do so, several carbon analogues were prepared. Phenylacetylene-terminated compounds **26a,b** were prepared according to a literature procedure from fluorenones **25a,b**[30] which are easily accessible from dibromofluorenones by coupling with phenylacetylene (see the Supporting Information). Compounds **25a,b** were treated with isopropylmag-

nesium chloride, and, after aqueous workup, the resulting alcohols were heated to reflux in acetic acid in the presence of about 0.15 equivalents of *p*-toluenesulfonic acid (*p*-TsOH) to afford acetylene-substituted 9-isopropylidene fluorenes **26a**,**b** (Scheme 4).

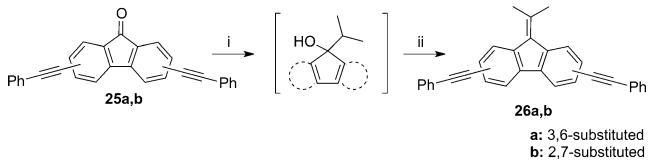

Scheme 4. i) *i*PrMgCl, THF, HCl; ii) *p*-TsOH, AcOH, reflux, 2 d.

X-ray crystallographic studies

The solid-state structures of representatives of each class of phosphaalkene-containing fluorenes as well as *C*,*C*-diphenyl phosphaalkenes were investigated by X-ray crystallography of crystals that were obtained by evaporation of binary or ternary solvent mixtures (CH_2Cl_2, MeOH, MeCN). The extended *C*,*C*-diphenyl phosphaalkene **24** crystallizes in the monoclinic space group $P2_1/n$. The P=C bond has a length of 1.699(2) Å, which lies in the expected range, and exhibits typical bending with a Mes*–P=C angle of 106.77(8)°. The deviation of the phenyl rings from the least-squares plane spanned by the C–P=C fragment with twist angles of 39.00(8)°and 41.29(8)° effectively disrupts π conjugation throughout the system (Figure 2). It can be assumed that a similar conformation persists also in solution, since it avoids steric clashes between the α protons of the two phenyl rings that would occur if the phenyl rings were coplanar.

2,7-Diacetylenic F9P **7b** also crystallizes in the monoclinic space group $P2_1/n$. The P=C bond length is slightly shorter (1.687(2) Å) with similar bending towards the Mes* group (106.2(1)°). Both phenyl rings of the fluorene and the P=C moiety span an almost perfect plane with maximum deviations of 0.063(3) Å and a twist angle of the phenyl rings of 1.0(1)°. Similarly, we obtained single crystals of **6a** as its methanol solvate in the triclinic space group $P\bar{1}$. The poorly defined methanol molecule around (1/2,1/2,1/2) was modeled with a positional disorder of the OH group. The phosphaalkene fragment shows similar structural parameters as in **7b** and **24** (P1–C1 1.693(2) Å and C30-P1-C1 103.25(11)°) and, as expected, high planarity of the F9P core (max. deviation 0.060(2) Å with a phenyl twist angle of 1.1(1)°). However, only one of the two terminal phenyl rings is nearly coplanar with the central moiety (7.4(1)°), whereas the other is twisted by 66.1(1)°.

Spectroscopic and theoretical investigations

Intrigued by previous studies on donor–acceptor systems built around fluorene cores, we were interested in the photophysi-

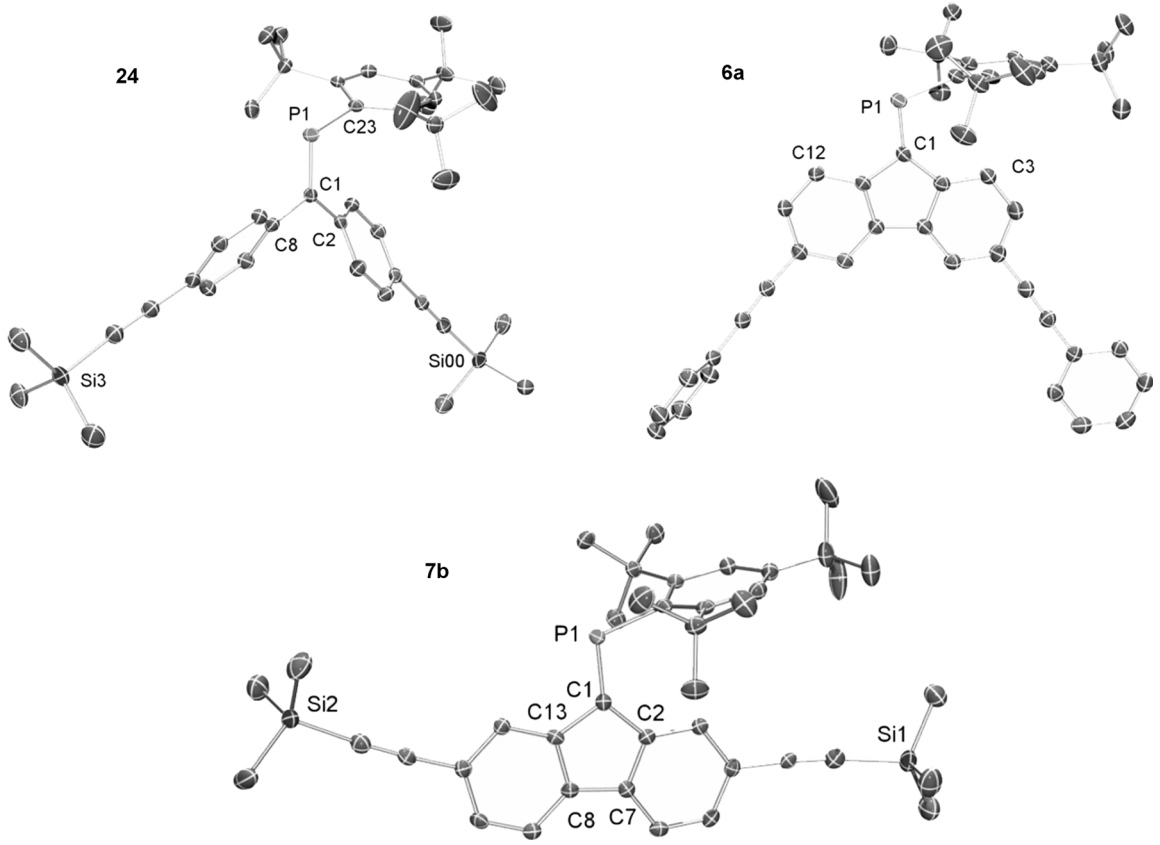

Figure 2. ORTEP plots[31] of compounds **24**, **6a**, and **7b** at 50% probability. Hydrogen atoms and solvent molecules are omitted for clarity. Structural and solution[32] details are given in the Supporting Information.

cal and electrochemical properties of the F9Ps in comparison with their all-carbon congeners. The different behavior of 2,7- versus 3,6-diacetylene-substituted fluorene-9-ylidene malononitrile derivatives has been discussed previously in terms of their different acceptor parts, that is, the malonitrile or fluorene unit.[12b]

UV/Vis spectroscopy

The influence of the exocyclic P center in the F9Ps on the electronic properties of the compounds becomes apparent on comparison of the UV/Vis spectra with those of the corresponding all-carbon-based dibenzofulvenes (Figure 3, top). Whereas the carbon analogue **26a** shows a broad absorption around 350 nm with a low-intensity feature reaching into the visible region, its P analogue **6a** has a prominent absorption at 400 nm. The effect of heteroatom incorporation is even more pronounced in the 2,7-disubstituted systems, for which the onset of absorption in the visible region is 524 nm for **6b**, as opposed to 395 nm for **26b**.

The UV/Vis spectroscopic data (Table 1) also allow evaluation of the effect of the acetylene groups and their position around the fluorene core. Not surprisingly, the non-acetylenic fluorene **10** exhibits the most blueshifted end absorption of the series, while introduction of a TMS-acetylene moiety in the 3-position of the fluorene, as in **17** ($\lambda_{max}=380$ nm), leads to a redshift of 12 nm. Introduction of a second TMS-acetylene moiety in the 6-position (**7a**) leads to an additional shift of 12 nm, and the longest-wavelength absorption maximum is observed at 392 nm.

The position of the acetylene substituents at the fluorene core significantly alters the optical properties of the compounds. The 2,7-disubstituted fluorene **6b** has a strong absorption around 354 nm with a shoulder at 382 nm and a long tail that extends far into the visible region ($\lambda_{onset}=524$ nm). In contrast, the longest-wavelength absorption maximum in the 3,6-disubstituted isomer **6a** is significantly redshifted with a broad maximum around 400 nm. It is clear from these results that the position of the acetylene groups at the fluorene core influences the degree to which they participate in the frontier molecular orbitals, as is discussed below.

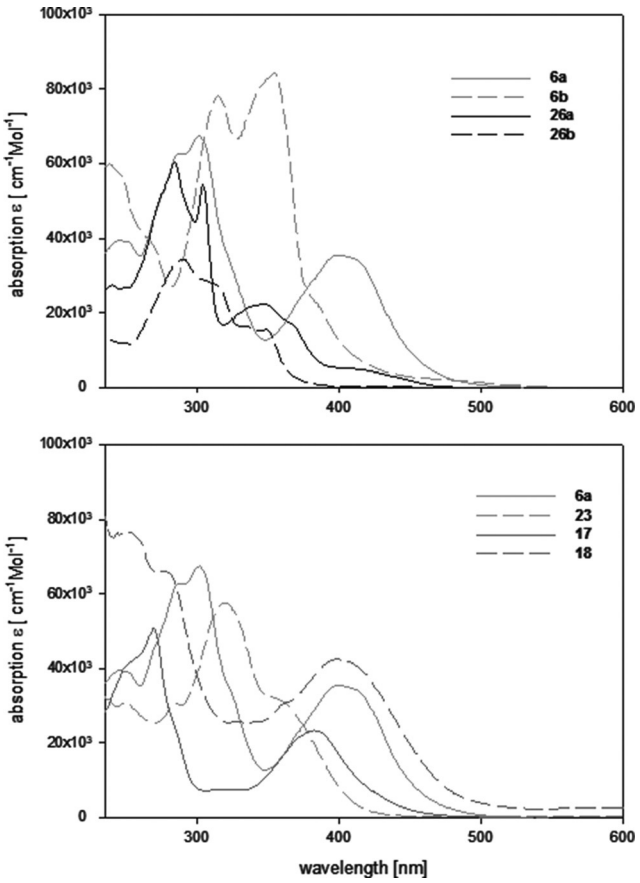

Figure 3. Top: UV/Vis absorption spectra of solutions of F9Ps **6a**,**b** and their carbon analogues **26a**,**b** in CH_2Cl_2. Bottom: comparison between the UV/Vis spectra (CH_2Cl_2) of F9P **6a** and its *C*,*C*-diphenyl phosphaalkene analogue **23**, and of the monoacetylenic F9P **17** and the butadiyne-bridged dimeric **18**.

The strongest effect on the optical properties of the compounds comes from the fluorene core itself, and is best illustrated by comparing fluorene **6a** with the *C*,*C*-diphenyl phosphaalkene **23**, which lacks the central C7–C8 bond. The lowest-energy absorption maximum of the latter is observed at 355 nm, that is, blueshifted by 45 nm compared to that of the former (Figure 3, bottom). A comparison of the monoacetylenic phosphaalkene **17** with its dimeric form **18** clearly indi-

Table 1. UV/Vis Spectroscopic and electrochemical data in CH_2Cl_2 at 25 °C. Electrochemical data for 1 mM solutions (0.1 M NBu_4PF_6) at $\nu=100$ mV s^{-1} (all potentials vs. $Fc^{+/0}$). Reversible peaks are given as their half-wave potentials [$E_{1/2}=(E_{pa}+E_{pc})/2$)], and irreversible peaks as the corresponding cathodic ($E_{p,c}$) or anodic peak potentials ($E_{p,a}$).

Compound	λ_{max} [nm] (ε [M^{-1}cm^{-1}])	Reduction $E_{1/2}$ [V]	Oxidation $E_{p,a}$ [V]
6a	400 (35500)	−1.74	1.04[b]
6b	354(84000), 385[a] (22000), 471[a] (2100)	−1.81	1.07[b]
7a	392 (7070)	−1.74	1.10[b]
7b	389 (24000)	−1.81	1.15[b]
10	368 (18200)	−1.99	1.06[b]
17	380 (23200)	−1.85	1.11[b]
23	317 (57100), 355[a] (32000)	−2.30[b]	0.95[b]
26a	347 (22200), 361[a] (18000), 410[a] (5000)	−2.36[b]	1.01[b] 1.21[b]
26b	352 (14500)	−2.41[b]	0.94[b]

[a] Shoulder. [b] Irreversible.

cates extended conjugation across the butadiyne unit, which shifts the maximum absorption by more than 20 nm from 380 to 404 nm.

TDDFT calculations

The most prominent bands in the UV/Vis spectra of the studied phosphaalkenes and their carbon analogues were assigned on the basis of time-dependent DFT (TDDFT) calculations. In all phosphaalkenes, the Mes* group was replaced by the electronically very similar 2,6-dimethylphenyl substituent (as indicated by a hash sign prior to each compound number). All structures were fully optimized at the B3LYP/6-311G* level of theory. Optimized structures were investigated with TDDFT at the same level of theory with consideration of ten states for singlets and triplets each. While the intense absorption in $^{\#}$**6b** at 400 nm is a single transition, two electronic transitions that involve the complete conjugated system contribute to the experimentally observed absorption in **26b** around 345 nm. In addition, there is a weaker absorption in $^{\#}$**6b** with a maximum of approximately 552 nm giving rise to its orange color (onset of 525 nm in the experimental UV spectrum of **6b**). This electronic transition has charge-transfer character, since the donor orbitals are mainly acetylene-based, whereas the accepting orbitals are predominantly located at the dibenzofulvenoid core of the molecule (Figure 4).[33]

The 3,6-disubstituted systems show a clear redshift for the maximum-wavelength absorptions compared to their 2,7-substituted congeners. Compound **26a** exhibits a broad maximum at around 350 nm with a clear shoulder extending into the visible region. In the case of $^{\#}$**6a**, we observed a similar situation with a broad feature around 400 nm with major contributions from a π–π^* and minor contributions from an n–π^* transition. Interestingly, a charge-transfer transition similar to that observed for $^{\#}$**6b** was observed neither experimentally nor by calculations for $^{\#}$**6a**.

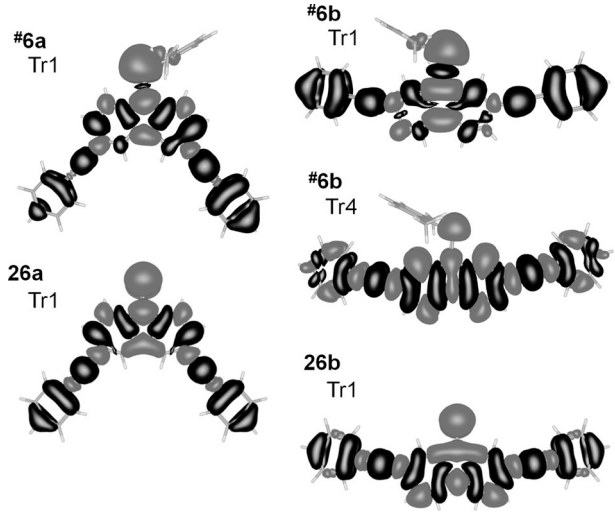

Figure 4. Electron-density difference maps of selected transitions. Isosurfaces were created with GaussSum[34] and plotted with GabeEdit at 99%. Dark isosurfaces correspond to electron depletion, and light gray isosurfaces indicate higher electron densities. $^{\#}$**6a** transition 1 [498 nm, HOMO−1→LUMO [78%], HOMO→LUMO (17%)]; **26a** transition 1 [405 nm, HOMO→LUMO (96%)]; $^{\#}$**6b** transition 1 [552 nm, HOMO→LUMO (96%)]; $^{\#}$**6b** transition 4 [380 nm, HOMO→LUMO+1 (98%)]; **26b** transition 1 [430 nm, HOMO→LUMO (90%)].

Electrochemistry

The redox properties of the F9Ps and their all-carbon congeners were examined by cyclic voltammetry. All observed trends are very similar for the TMS- and phenyl-terminated alkynes, and hence only the latter are discussed in detail. In addition, first-principles calculations were performed on the compounds and the results correlated to the experimental findings. Together, it emerged that an interplay between the different acetylene substitution patterns and heteroatom incorporation dictates the electrochemical properties of the compounds.

All F9Ps show a reversible reduction between −1.7 and −2.0 V versus ferrocenium/ferrocene ($Fc^{+/0}$), and the parent F9P **10** exhibits the most negative reduction potential ($E_{1/2}$ = −1.99 V) of the series (Figure 5), which is attributed to the formation of the anionic fulvenoid with phosphinyl radical. The CVs of the all-carbon reference compounds **26a**,**b** and diphenyl phosphaalkene **23** show only nonreversible reductions that can be observed at considerably more negative potentials (Supporting Information).[15b]

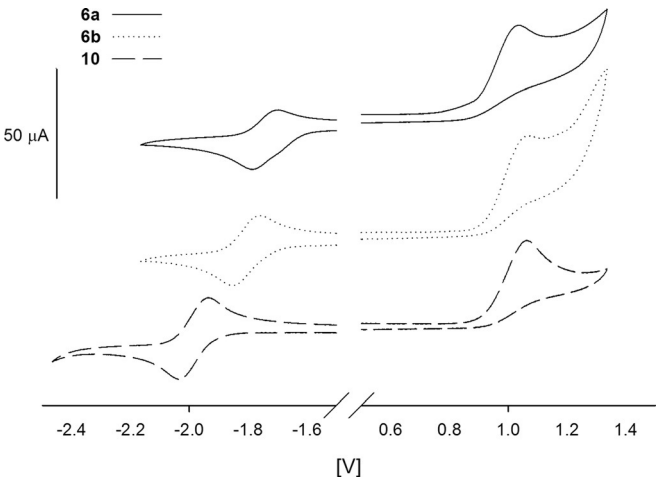

Figure 5. Cyclic voltammograms of compounds **6a**,**b** and unsubstituted F9P **10**. (1 mM in CH_2Cl_2, 0.1 M NBu_4PF_6, ν = 100 mV s^{-1}, vs. $Fc^{+/0}$).

Calculations on **6a**,**b** and **26a**,**b**, showed that the LUMOs are an antibonding combination of the entire fluorene/dibenzofulvene core (including the exocyclic double bond) with partial contributions from the phenylacetylene fragments (Figure 6), irrespective of the position of the acetylene substituents. Incorporation of the heteroelement in **6b** leads to significant stabilization of the LUMO compared to that of its all-carbon congener **26b** ($^{\#}$**6b**: −2.75 eV versus **26b**: −2.20 eV), which explains the cathodically shifted reduction potential for the latter compound. A similar situation of LUMO energies and shapes is found for the 3,6-substituted compounds **6a** and **26a**. Com-

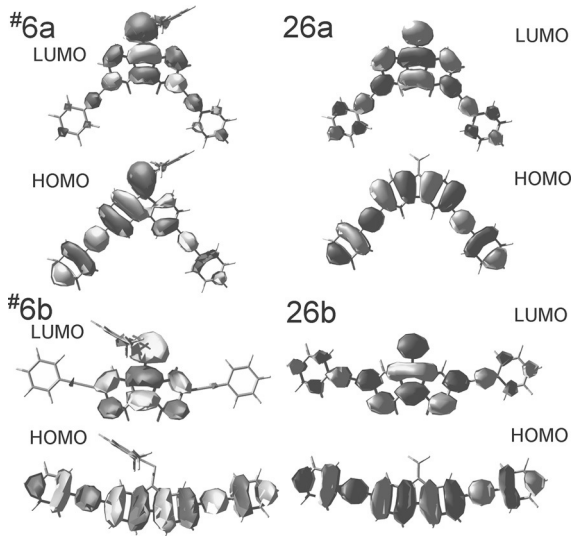

Figure 6. Frontier molecular orbitals of F9Ps **#6a,b** and their C analogues **26a,b**. Calculated at the B3LYP/6-311G* level of theory.

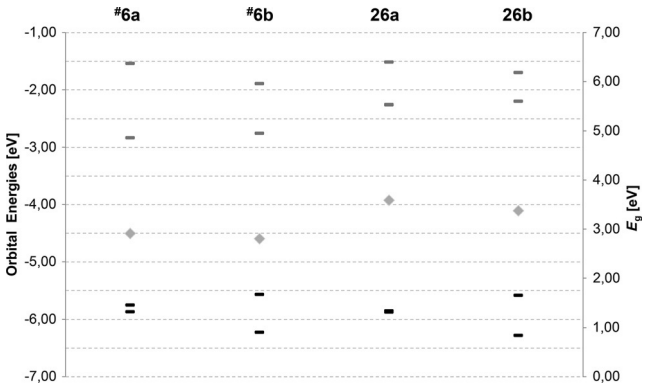

Figure 7. Calculated orbital energies and HOMO–LUMO splittings E_g for model systems **#6a,b** and **26a,b**. Black and gray bars denote occupied and empty orbitals, respectively. The secondary axis (gray diamonds) is the HOMO–LUMO splitting. All values are given in electron volts.

paring the LUMOs of **6a** and **6b** (Figure 6) suggests that the 3,6 substitution pattern allows a larger contribution from the acetylene units, which gives rise to increased delocalization that can be even detected in the reduction potentials in the respective CVs, which differ by 70 mV.

In the anodic scan, the differences in the CVs of **6a,b** and **26a,b** are more subtle. DFT investigations showed that, in the case of 2,7 substitution, the HOMO extends over the π systems of the phenylacetylene moieties and the fluorene core, but excludes the pπ orbitals of the exocyclic double bond. In the absence of any contribution from the exocyclic double bond, the energies of the Kohn–Sham orbitals are very similar for **#6b** and **26b** (−5.56 and −5.58 eV, respectively). In contrast, the HOMO of **6a** is significantly different to that of its carbon analogue **26a**, as the HOMO of the former is rather asymmetric and mainly localized on the side of the molecule that is opposite to the bulky *P*-substituent (Figure 6). As a consequence, the extent of π conjugation is decreased. In contrast to the situation in **26a** and the 2,7-disubstituted compounds **#6b** and **26b**, the HOMO in **#6a** has contributions from the pπ orbitals of the exocyclic phosphaalkene. Notably, this stabilization counterbalances the destabilization that is caused by the more localized π conjugation, and the calculated orbital energies are rather similar for both **#6a** (−5.74 eV) and **26a** (−5.85 eV). This finding is also corroborated by the very similar experimental oxidation potentials (Table 1 and Supporting Information).

Comparing the phenyl-terminated **6a,b** with the TMS-terminated F9Ps **7a,b** shows that the phenyl termini in the former compounds do not participate in the LUMOs, as the experimentally observed reduction potentials are literally identical. In contrast, the oxidation potentials are significantly shifted to milder potentials when the phenyl termini are present, which indicates a sizable contribution of the phenyl-based π system to the HOMOs of the compounds.

Figure 7 summarizes the results for the calculated model compounds **#6a,b** and their carbon analogues **26a,b**. The experimentally observed decrease of the HOMO–LUMO gaps (by UV/Vis onsets and CV experiments) for the phosphaalkene derivatives is caused by a significant stabilization of the LUMO levels, whereas the HOMO levels are almost unaltered in the C and the P compounds. Consequently, the calculated static HOMO–LUMO splittings E_g for the fluorene-9-ylidene phosphanes are between 2.8 and 2.9 eV, whereas their carbon analogues show E_g values between 3.4 and 3.6 eV.

Conclusion

We have developed flexible synthetic procedures for diacetylenic F9Ps. The synthetic versatility of compounds with TMS-acetylene moieties was demonstrated by protodesilylation reactions to afford the terminal acetylenes, which could then be further elaborated by Sonogashira cross-coupling or Glaser-type homocoupling reactions to afford bis-thienyl-functionalized compounds and a butadiyne-bridged dimer, respectively.

Most intriguing are the significant differences in the frontier molecular orbitals depending on heteroelement substitution and variation of the acetylene substitution patterns. The presence of the P center causes a significant decrease in the HOMO–LUMO splitting, as evidenced by UV/Vis spectroscopy and cyclic voltammetry, and corroborated by DFT calculations. The fluorene-9-ylidene phosphanes presented herein thus open new possibilities for highly planar systems that incorporate an exocyclic phosphaethene unit as new functional building block for low-bandgap materials.

Variation of the substitution patterns around the fluorene core leads to significant changes in optical and electronic properties. Whereas 3,6-disubstituted compounds have strong absorptions around 400 nm, mainly due to π–π* transitions, 2,7-diacetylenic F9Ps exhibit longest-wavelength absorptions that have significant charge-transfer (CT) character with an onset around 520 nm. Such transitions are highly desirable for the construction of future donor–acceptor arrays based on the fluorene core, as previously described for classical all-carbon fluorenes.[12b,35] Further enhancement of the CT character is the subject of ongoing work.

Experimental Section

Synthetic procedures were carried out under an inert atmosphere by using modified Schlenk techniques unless otherwise stated. Reagents were obtained from commercial suppliers and used as received. Solvents were freshly distilled over sodium or CaH_2. NMR spectra were recorded with a JEOL Eclipse+ spectrometer operating at a proton frequency of 400 MHz or a Varian Unity Innova instrument operating at a proton frequency of 300 MHz. The spectra were referenced internally to residual solvent peaks (^{1}H and ^{13}C NMR) or externally to 85% aqueous H_3PO_4 (^{31}P NMR).

[3,6-Bis(phenylethynyl)-(9*H*-fluoren-9-ylidene)](2,4,6-tri-tert-butylphenyl)phosphane (6a)

A solution of *n*BuLi (2.5 M in hexane, 0.52 mmol, 0.21 mL) was added dropwise at −78 °C to a stirred solution of substituted fluorene **2a** (183 mg, 0.5 mmol) in THF (3 mL) and the reaction mixture was stirred for 0.5 h. This solution was slowly transferred via cannula to a solution of Mes*PCl_2 (0.5 mmol, 0.174 g) in THF (4 mL) cooled to −78 °C and the reaction mixture was stirred for 1 h. After this, a solution of DBU (1 M in THF, 0.75 mmol, 0.75 mL) was added and the reaction mixture was allowed to warm to room temperature. The reaction mixture was passed through a pad of silica and all volatile substances were evaporated. The solid residue was purified by chromatography on silica with 10% toluene in hexane. Yield: 144 mg, 45%. ^{1}H NMR (300 MHz, $CDCl_3$): δ = 8.25 (dd, $^3J_{HH}$ = 8.0 Hz, $^4J_{PH}$ = 4.3 Hz, 1H), 7.83 (br s, 1H), 7.76 (s, 1H), 7.68–7.46 (m, 7H), 7.46–7.30 (m, 6H), 6.91 (dd, $^3J_{HH}$ = 8.2 Hz, $^4J_{HH}$ = 1.2 Hz, 1H), 5.00 (dd, $^3J_{HH}$ = 8.2 Hz, $^4J_{PH}$ = 2.6 Hz, 1H), 1.48 (s, 9H), 1.45 (s, 18H); ^{13}C NMR (75 MHz, $CDCl_3$): δ = 168.9 (d, $^1J_{CP}$ = 44 Hz, P=C), 154.6 (*o*-Mes*), 152.1 (*p*-Mes*), 143.2 (d, $^2J_{CP}$ = 27 Hz, Ar), 138.9 (d, J_{CP} = 11 Hz, Ar), 138.3 (d, $^2J_{CP}$ = 17 Hz, Ar), 137.7 (d, J_{CP} = 14 Hz, Ar), 134.4 (d, $^1J_{CP}$ = 57 Hz, *i*-Mes*), 131.9 (Ar), 131.8 (Ar), 130.8 (J_{CP} = 2 Hz, Ar), 130.6 (J_{CP} = 4 Hz, Ar), 128.7 (Ar), 128.6 (Ar), 128.5 (Ar), 126.4 (J_{CP} = 7 Hz, Ar), 123.6 (Ar), 123.5 (Ar), 123.04 (*m*-Mes*), 122.98 (Ar), 122.9 (Ar), 122.5 (J_{CP} = 2 Hz, Ar), 120.7 (d, J_{CP} = 24 Hz, Ar), 91.0 (J_{CP} = 3 Hz, C≡C), 90.6 (br, C≡C), 90.3 (J_{CP} = 3 Hz, C≡C), 38.5 (*t*Bu), 35.5 (*t*Bu), 33.0 (J_{CP} = 7 Hz, *t*Bu), 31.8 (*t*Bu); ^{31}P NMR (121 MHz, $CDCl_3$): δ = 267.3; HRMS [solution in $CHCl_3$/MeOH, silver trifluoroacetate (AgTFA)] calcd for $(C_{47}H_{45}P)_2Ag$ $[2M+Ag]^+$: 1389.5586; found: 1389.5584.

[3,6-Bis(thiophen-2-ylethynyl)-(9*H*-fluoren-9-ylidene)](2,4,6-tri-*tert*-butylphenyl)phosphane (9a)

Compound **9a** was synthesized in analogy to the literature procedure.[20f] $[Pd(PPh_3)_2Cl_2]$ (0.03 mmol, 22 mg), CuI (0.06 mmol, 12 mg), and aqueous K_2CO_3 (2 M, 1.5 mL) were added successively to a degassed solution of **7a** (0.32 mmol, 0.2 g) and 2-iodothiophene (0.63 mmol, 0.13 g) in THF (20 mL), MeOH (10 mL), and Et_3N (5 mL) under an argon atmosphere. The reaction was monitored by TLC (2% EtOAc in hexane) and quenched after completion by the addition of brine (10 mL) after approximately 20 h. The reaction mixture was extracted with EtOAc (3×50 mL) and the combined organic phases were dried over $MgSO_4$ and concentrated in vacuo. The product was purified by column chromatography (silica, 5% EtOAc in hexane). Yield: 0.08 g, 38%. ^{1}H NMR (400 MHz, $CDCl_3$): δ = 8.22 (dd, $^3J_{HH}$ = 7.8 Hz, $^4J_{PH}$ = 3.8 Hz, 1H), 7.78 (s, 1H), 7.71 (s, 1H), 7.57 (s, 2H), 7.47 (dd, $^3J_{HH}$ = 8.0 Hz, $^4J_{PH}$ = 1.1 Hz, 1H), 7.37–7.20 (m, 5H), 7.02 (m, 2H), 6.87 (dd, $^3J_{HH}$ = 8.2 Hz, $^4J_{HH}$ = 1.2 Hz, 1H), 5.00 (d, $^3J_{HH}$ = 7.9 Hz, 1H), 1.46 (s, 9H), 1.42 (s, 18H); ^{13}C NMR (100 MHz, $CDCl_3$): δ = 168.5 (d, $^1J_{CP}$ = 44 Hz, P=C), 154.4 (*o*-Mes*), 152.0 (*p*-Mes*), 143.1 (d, $^2J_{CP}$ = 27 Hz, Ar), 138.6 (d, J_{CP} = 10 Hz, Ar), 138.2 (d, $^2J_{CP}$ = 17 Hz, Ar), 137.5 (d, J_{CP} = 15 Hz, Ar), 134.2 (d, $^1J_{CP}$ = 57 Hz, *i*-Mes*), 132.1 (Ar), 132.0 (Ar), 130.4 (J_{CP} = 2 Hz, Ar), 130.2 (J_{CP} = 4 Hz, Ar), 127.5 (Ar), 127.4 (Ar), 127.3 (Ar), 126.2 (J_{CP} = 7 Hz, Ar), 123.6 (Ar), 123.4 (Ar), 122.9 (*m*-Mes*), 122.6 (Ar), 122.5 (J_{CP} = 8 Hz, Ar), 122.4 (d, J_{CP} = 7 Hz, Ar), 122.1 (d, J_{CP} = 3 Hz, Ar) 120.5 (d, J_{CP} = 24 Hz, Ar), 94.1 (J_{CP} = 2 Hz, C≡C), 93.8 (J_{CP} = 3 Hz, C≡C), 84.1 (J_{CP} = 2 Hz, C≡C), 83.6 (J_{CP} = 2 Hz, C≡C), 38.3 (*t*Bu), 35.3 (*t*Bu), 32.9 (J_{CP} = 7 Hz, *t*Bu), 31.7 (*t*Bu); ^{31}P NMR (161 MHz, $CDCl_3$): δ = 268.1; HRMS (solution in $CHCl_3$/ACN, AgTFA) calcd for $C_{43}H_{41}PS_2Ag$ $[M+Ag]^+$: 761.1433; found: 761.1429.

{Bis[4-(phenylethynyl)phenyl]methylene}(2,4,6-tri-*tert*-butylphenyl)phosphane (23)

A solution of *n*BuLi (2.5 M in hexane, 0.52 mmol, 0.21 mL) was added dropwise at −78 °C to a stirred solution of diphenylmethane **19** (184 mg, 0.5 mmol) in THF (3 mL), and the reaction mixture was stirred for 0.5 h. The resulting solution was added dropwise via cannula to a solution of Mes*PCl_2 (0.5 mmol, 0.174 g) in THF (4 mL) at −78 °C and the reaction mixture was stirred for 1 h. After this, the solvent was removed in vacuo. The residue was dissolved in dry toluene (10 mL) and a solution of DBU (1 M in THF, 0.75 mmol, 0.75 mL) was added. The reaction mixture was heated to reflux for 48 h. After cooling to room temperature the reaction mixture was passed through a pad of silica and all volatile substances were evaporated. The solid residue was purified by chromatography on silica with 20% toluene in hexane. Yield: 48 mg, 15%. ^{1}H NMR (300 MHz, $CDCl_3$): δ = 7.61–7.45 (m, 6H), 7.45–7.28 (m, 10H), 7.04 (d, $^3J_{HH}$ = 8.4 Hz, 2H), 6.40 (dd, $^3J_{HH}$ = 8.4 Hz, $^4J_{PH}$ = 1.3 Hz, 2H), 1.50 (s, 18H), 1.38 (s, 9H); ^{13}C NMR (75 MHz, $CDCl_3$): δ = 178.7 (d, $^1J_{CP}$ = 47 Hz, P=C), 154.9 (*o*-Mes*), 151.3 (*p*-Mes*), 145.7 (d, $^2J_{CP}$ = 28 Hz, Ar), 142.2 (d, $^2J_{CP}$ = 17 Hz, Ar), 135.5 (d, $^1J_{CP}$ = 62 Hz, *i*-Mes*), 131.9 (Ar), 131.81 (Ar), 131.76 (Ar), 130.6 (d, J_{CP} = 2 Hz, Ar), 129.4 (d, $^3J_{CP}$ = 7 Hz, Ar), 129.0 (d, $^3J_{CP}$ = 18.6 Hz, Ar), 128.61 (Ar), 128.58 (Ar), 128.52 (Ar), 128.49 (Ar), 123.6 (Ar), 123.5 (Ar), 123.0 (d, J_{CP} = 4 Hz, Ar), 122.3 (*m*-Mes*), 121.7 (d, J_{CP} = 3 Hz, Ar), 90.7 (C≡C), 90.3 (C≡C), 89.8 (C≡C), 89.7 (C≡C), 38.4 (*t*Bu), 35.3 (*t*Bu), 33.4 (d, J_{CP} = 7 Hz, *t*Bu), 31.8 (*t*Bu); ^{31}P NMR (121 MHz, $CDCl_3$): δ = 251.6; HRMS (solution in $CHCl_3$/MeOH, AgTFA) calcd for $(C_{47}H_{47}P)_2Ag$ $[2M+Ag]^+$: 1393.5900; found: 1397.5894.

Acknowledgements

The Swedish Research Council, the Göran Gustafsson Foundation, COST action CM1302 SIPs, the Lars-Hiertas Memorial Fund (FO2014-0024), and Uppsala University (U3MEC molecular electronics priority initiative) are greatly acknowledged for financial support. The authors would like to thank Dr. A. I. Arkhypchuk for fruitful discussions. Y.V.S. is grateful to the Swedish Institute for a scholarship in the Visby Program (382/00386/2012). A.O. acknowledges the Austrian Science Funds (FWF, Project J3193-N17).

Keywords: alkynes · conjugation · electrochemistry · fluorenes · phospaalkenes

[1] U. H. F. Bunz, *Chem. Rev.* **2000**, *100*, 1605 – 1644.

[2] a) M. B. Nielsen, F. Diederich, *Chem. Rev.* **2005**, *105*, 1837 – 1868; b) F. Diederich, P. J. Stang, R. R. Tykwinski, *Acetylene Chemistry*, Wiley-VCH, Weinheim, **2005**; c) S. Ott, R. Faust, *Chem. Commun.* **2004**, 388 – 389.

[3] a) A. R. Murphy, J. M. J. Fréchet, *Chem. Rev.* **2007**, *107*, 1066 – 1096; b) A. C. Grimsdale, K. Leok Chan, R. E. Martin, P. G. Jokisz, A. B. Holmes, *Chem. Rev.* **2009**, *109*, 897 – 1091; c) B. B. Carbas, D. Asil, R. H. Friend, A. M. Önal, *Org. Electron.* **2014**, *15*, 500 – 508.
[4] S. H. Lee, T. Nakamura, T. Tsutsui, *Org. Lett.* **2001**, *3*, 2005 – 2007.
[5] M. Iyoda, H. Otani, M. Oda, *Angew. Chem. Int. Ed. Engl.* **1988**, *27*, 1080 – 1081; *Angew. Chem.* **1988**, *100*, 1131 – 1132.
[6] M. Kreyenschmidt, G. Klaerner, T. Fuhrer, J. Ashenhurst, S. Karg, W. D. Chen, V. Y. Lee, J. C. Scott, R. D. Miller, *Macromolecules* **1998**, *31*, 1099 – 1103.
[7] J. Lewis, P. R. Raithby, W.-Y. Wong, *J. Organomet. Chem.* **1998**, *556*, 219 – 228.
[8] X. Gu, J. Yao, G. Zhang, D. Zhang, *Small* **2012**, *8*, 3406 – 3411.
[9] T. Nakano, K. Takewaki, T. Yade, Y. Okamoto, *J. Am. Chem. Soc.* **2001**, *123*, 9182 – 9183.
[10] H. Kong, D. H. Lee, I.-N. Kang, E. Lim, Y. K. Jung, J.-H. Park, T. Ahn, M. H. Yi, C. E. Park, H.-K. Shim, *J. Mater. Chem.* **2008**, *18*, 1895 – 1902.
[11] S. Gélinas, J. Kirkpatrick, I. A. Howard, K. Johnson, M. W. B. Wilson, G. Pace, R. H. Friend, C. Silva, *J. Phys. Chem. B* **2012**, *116*, 4649 – 4653.
[12] a) C. Du, C. Li, W. Li, X. Chen, Z. Bo, C. Veit, Z. Ma, U. Wuerfel, H. Zhu, W. Hu, F. Zhang, *Macromolecules* **2011**, *44*, 7617 – 7624; b) L. A. Estrada, D. C. Neckers, *J. Org. Chem.* **2009**, *74*, 8484 – 8487; c) N. Fomina, S. E. Bradforth, T. E. Hogen-Esch, *Macromolecules* **2009**, *42*, 6440 – 6447.
[13] N. Fomina, T. E. Hogen-Esch, *Macromolecules* **2008**, *41*, 3765 – 3768.
[14] S. Yao, K. D. Belfield, *J. Org. Chem.* **2005**, *70*, 5126 – 5132.
[15] a) L. A. Estrada, X. Cai, D. C. Neckers, *J. Phys. Chem. A* **2011**, *115*, 2184 – 2195; b) L. A. Estrada, J. E. Yarnell, D. C. Neckers, *J. Phys. Chem. A* **2011**, *115*, 6366 – 6375; c) I. F. Perepichka, A. F. Popov, T. V. Orekhova, M. R. Bryce, A. N. Vdovichenko, A. S. Batsanov, L. M. Goldenberg, J. A. K. Howard, N. I. Sokolov, J. L. Megson, *J. Chem. Soc. Perkin Trans. 2* **1996**, *0*, 2453 – 2469; d) I. F. Perepichka, A. F. Popov, T. V. Orekhova, M. R. Bryce, A. M. Andrievskii, A. S. Batsanov, J. A. K. Howard, N. I. Sokolov, *J. Org. Chem.* **2000**, *65*, 3053 – 3063.
[16] a) A. Fukazawa, S. Yamaguchi, *Chem. Asian J.* **2009**, *4*, 1386 – 1400; b) M. Hissler, P. W. Dyer, R. Reau, *Coord. Chem. Rev.* **2003**, *244*, 1 – 44; c) J. I. Bates, J. Dugal-Tessier, D. P. Gates, *Dalton Trans.* **2010**, *39*, 3151 – 3159; d) T. Baumgartner, *Acc. Chem. Res.* **2014**, *47*, 1613 – 1622.
[17] a) A. Patra, Y. H. Wijsboom, L. J. W. Shimon, M. Bendikov, *Angew. Chem. Int. Ed.* **2007**, *46*, 8814 – 8818; *Angew. Chem.* **2007**, *119*, 8970 – 8974; b) C. Booker, X. Wang, S. Haroun, J. Zhou, M. Jennings, B. L. Pagenkopf, Z. Ding, *Angew. Chem. Int. Ed.* **2008**, *47*, 7731 – 7735.
[18] a) T. Baumgartner, R. Réau, *Chem. Rev.* **2006**, *106*, 4681 – 4727; b) X. He, J. Borau-Garcia, A. Y. Y. Woo, S. Trudel, T. Baumgartner, *J. Am. Chem. Soc.* **2013**, *135*, 1137 – 1147; c) W. Shen, S. Graule, J. Crassous, C. Lescop, H. Gornitzka, R. Reau, *Chem. Commun.* **2008**, 850 – 852; d) H. Chen, S. Pascal, Z. Wang, P.-A. Bouit, Z. Wang, Y. Zhang, D. Tondelier, B. Geffroy, R. Réau, F. Mathey, Z. Duan, M. Hissler, *Chem. Eur. J.* **2014**, *20*, 9784 – 9793; e) F. Riobé, R. Szűcs, P.-A. Bouit, D. Tondelier, B. Geffroy, F. Aparicio, J. Buendía, L. Sánchez, R. Réau, L. Nyulászi, M. Hissler, *Chem. Eur. J.* **2015**, *21*, 6547 – 6556; f) V. B. Gudimetla, L. Ma, M. P. Washington, J. L. Payton, M. C. Simpson, J. D. Protasiewicz, *Eur. J. Inorg. Chem.* **2010**, 854 – 865; g) Y. Matano, A. Saito, T. Fukushima, Y. Tokudome, F. Suzuki, D. Sakamaki, H. Kaji, A. Ito, K. Tanaka, H. Imahori, *Angew. Chem. Int. Ed.* **2011**, *50*, 8016 – 8020; *Angew. Chem.* **2011**, *123*, 8166 – 8170.
[19] H. Kawanami, K. Toyota, M. Yoshifuji, *J. Organomet. Chem.* **1997**, *535*, 1 – 5.
[20] a) V. B. Gudimetla, A. L. Rheingold, J. L. Payton, H.-L. Peng, M. C. Simpson, J. D. Protasiewicz, *Inorg. Chem.* **2006**, *45*, 4895 – 4901; b) R. C. Smith, X. Chen, J. D. Protasiewicz, *Inorg. Chem.* **2003**, *42*, 5468 – 5470; c) C. Moser, A. Orthaber, M. Nieger, F. Belaj, R. Pietschnig, *Dalton Trans.* **2006**, 3879 – 3885; d) B. Schäfer, E. Öberg, M. Kritikos, S. Ott, *Angew. Chem. Int. Ed.* **2008**, *47*, 8228 – 8231; *Angew. Chem.* **2008**, *120*, 8352 – 8355; e) X.-L. Geng, Q. Hu, B. Schäfer, S. Ott, *Org. Lett.* **2010**, *12*, 692 – 695; f) X.-L. Geng, S. Ott, *Chem. Eur. J.* **2011**, *17*, 12153 – 12162; g) C. Moser, M. Nieger, R. Pietschnig, *Organometallics* **2006**, *25*, 2667 – 2672; h) A. Orthaber, F. Belaj, R. Pietschnig, *Inorg. Chim. Acta* **2011**, *374*, 211 – 215.
[21] a) H. Miyake, T. Sasamori, J. I. C. Wu, P. v. R. Schleyer, N. Tokitoh, *Chem. Commun.* **2012**, *48*, 11440 – 11442; b) H. Miyake, T. Sasamori, N. Tokitoh, *Angew. Chem.* **2012**, *124*, 3514 – 3517.
[22] a) A. Decken, C. J. Carmalt, J. A. C. Clyburne, A. H. Cowley, *Inorg. Chem.* **1997**, *36*, 3741 – 3744; b) T. A. D. Van Knaap, F. Bickelhaupt, *Chem. Ber.* **1984**, *117*, 915 – 924; c) G. Märkl, K. M. Raab, *Tetrahedron Lett.* **1989**, *30*, 1077 – 1080; d) N. Burford, T. S. Cameron, J. A. C. Clyburne, K. Eichele, K. N. Robertson, S. Sereda, R. E. Wasylishen, W. A. Whitla, *Inorg. Chem.* **1996**, *35*, 5460 – 5467.
[23] A. I. Arkhypchuk, Y. V. Svyaschenko, A. Orthaber, S. Ott, *Angew. Chem. Int. Ed.* **2013**, *52*, 6484 – 6487; *Angew. Chem.* **2013**, *125*, 6612 – 6615.
[24] a) S. Kawasaki, A. Nakamura, K. Toyota, M. Yoshifuji, *Bull. Chem. Soc. Jpn.* **2005**, *78*, 1110 – 1120; b) K. Toyota, S. Kawasaki, A. Nakamura, M. Yoshifuji, *Chem. Lett.* **2003**, *32*, 430 – 431.
[25] a) A. Al Badri, M. Chentit, M. Geoffroy, A. Jouaiti, *J. Chem. Soc. Faraday Trans.* **1997**, *93*, 3631 – 3635; b) X. Pan, X. Wang, Y. Zhao, Y. Sui, X. Wang, *J. Am. Chem. Soc.* **2014**, *136*, 9834 – 9837.
[26] E. Öberg, X.-L. Geng, M.-P. Santoni, S. Ott, *Org. Biomol. Chem.* **2011**, *9*, 6246 – 6255.
[27] Z. Wu, Y. Xiong, J. Zou, L. Wang, J. Liu, Q. Chen, W. Yang, J. Peng, Y. Cao, *Adv. Mater.* **2008**, *20*, 2359 – 2364.
[28] B. W. Rawe, C. P. Chun, D. P. Gates, *Chem. Sci.* **2014**, *5*, 4928 – 4938.
[29] X.-L. Geng, S. Ott, *Chem. Commun.* **2009**, 7206 – 7208.
[30] S. Fujisaki, Y. Nakashige, A. Nishida, S. Kajigaeshi, H. Hara, *Nippon Kagaku Kaishi* **1983**, *1983*, 1059 – 1063.
[31] L. J. Farrugia, *J. Appl. Crystallogr.* **1997**, *30*, 565.
[32] a) G. Sheldrick, *Acta Crystallogr. Sect. A* **2015**, *71*, 3 – 8; b) G. Sheldrick, *Acta Crystallogr. Sect. A* **2008**, *64*, 112 – 122.
[33] The calculated UV transitions are generally shifted to lower energies compared to experimental UV spectra.
[34] N. M. O'Boyle, A. L. Tenderholt, K. M. Langner, *J. Comput. Chem.* **2008**, *29*, 839 – 845.
[35] S. Karak, P. J. Homnick, L. A. Renna, D. Venkataraman, J. T. Mague, P. M. Lahti, *ACS Appl. Mater. Interfaces* **2014**, *6*, 16476 – 16480.

Received: August 28, 2015
Published online on February 2, 2016